Swarm and Evolutionary Computation 47 (2019) 89–95

Contents lists available at ScienceDirect

Swarm and Evolutionary Computation

journal homepage: www.elsevier.com/locate/swevo

Multimodal continuous ant colony optimization for multisensor remote sensing image registration with local search

Yue Wu[a,*], Wenping Ma[b], Qiguang Miao[a], Shanfeng Wang[b]

[a] School of Computer Science and Technology, Xidian University, Xi'an, Shaanxi Province 710071, China
[b] Key Laboratory of Intelligent Perception and Image Understanding of Ministry of Education, International Research Center for Intelligent Perception and Computation, Joint International Research Laboratory of Intelligent Perception and Computation, Xidian University, Xi'an, Shaanxi Province 710071, China

ARTICLE INFO

Keywords:
Image registration
Remote sensing
Ant colony optimization
Local search

ABSTRACT

Due to the large differences between different imaging sensors, multisensor remote sensing image registration is a challenging work. Multisensor remote sensing image registration can be formulated as a multimodal problem, and general optimization methods may get trapped into a local optimum when solving complex multimodal problems. In this paper, we introduce a multimodal continuous ant colony optimization algorithm for multisensor remote sensing image registration, and an efficient optimization method is designed as local search operation. Multimodal continuous ant colony optimization algorithm can preserve high diversity and has the global search ability for multimodal problems. Meanwhile, efficient local search operation can improve the efficiency and provide the accurate result. The experimental results have demonstrated the effectiveness and robustness of the proposed method.

1. Introduction

Remote sensing image registration is one of the fundamental tasks in remote sensing image processing [3,47]. Image registration aims to align two or more images into same coordinate system, and overlapping area is usually the area of interest [2,34]. It is an important step for many remote sensing image processing procedures, such as image fusion [19], object recognition [26], change detection [13], etc. The performance of image registration has large influence on the performance of the follow-up procedure [4]. So the accurate result of remote sensing image registration is necessary [41].

In the literature, remote sensing image registration methods can be coarsely partitioned into two categories: feature-based and intensity-based [47]. Feature-based methods extract corresponding features (point, line and region), and obtain the geometric transformation through the matched features [45]. In [14], edge information is used to increase multitemporal image registration accuracy. And region feature can also be used for fine registration of very high resolution multitemporal images [15]. The most famous feature for image registration is scale-invariant feature transform algorithm (SIFT) [27], and a lot of corresponding remote sensing versions have been proposed, such as SAR-SIFT [6], PSO-SIFT [28], etc. These features play an important role in feature-based methods [20]. On the other hand, the intensity of the images is used as similarity measure in intensity-based methods [12]. The intensity-based methods usually contain two procedures: similarity measure and optimization algorithm [18]. The similarity measure is the key procedure in the intensity-based methods, because appropriate similarity measure directly influences the registration result. A lot of similarity measures have been proposed, such as sum-of-squared-differences (SSD), correlation coefficient (CC) [17], mutual information (MI) [29], and differential total variation (DTV) [22,21]. MI is one of the most famous similarity measures, and it is widely used in image registration [23]. DTV is one of the best similarity measures, which is based on the differential total variation in the gradient domain [21]. In practice, due to the large differences of the imaging sensors, registration of multisensor remote sensing image is difficult [44]. Although some methods have been proposed, multisensor remote sensing image registration is still a challenging work [30]. As shown in Fig. 1, two multisensor images are registered through MI, and we can see that it is a multimodal problem [42]. There are a lot of local optima, and it is difficult to find the correct result. General optimization methods are usually designed for unimodal problem, which may be invalid for some multimodal problems. Multimodal optimization method is designed for multimodal problem, so it will be efficient and robust for multimodal problem.

Ant colony optimization (ACO), which is inspired by the foraging behavior of ant in the nature, is a novel heuristic approach in evolutionary computation [9]. Ants are able to find the shortest path

* Corresponding author.
E-mail address: ywu@xidian.edu.cn (Y. Wu).

http://dx.doi.org/10.1016/j.swevo.2017.07.004
Received 15 March 2017; Received in revised form 7 June 2017; Accepted 6 July 2017
Available online 08 July 2017

Fig. 1. An multisensor remote sensing image registration example with MI. (a) Optical image. (b) SAR image. (c) Similarity measure of MI.

from the food source to their nest over time by communicating with each other instead of visual cues [8]. Ants can deposit chemical information according to the distance of the path [36], and we call this chemical information pheromones [7]. Different from other evolutionary algorithms, ACO algorithm is a reactive search optimization method adopting the principle of "learning while optimizing" [43]. ACO is originally proposed for discrete problems, and has solved a lot of discrete problems effectively [32,37]. Due to its high performance [1,16], ACO algorithm has been extended to a continuous version (ACO_R) to solve continuous problems [38]. In ACO_R, solutions are constructed through Gaussian kernel function. This solution construction strategy can maintain high diversity, and it is efficient for multimodal optimization [46]. Then, an adaptive multimodal continuous ACO algorithm (AM-ACO) is proposed, and it performs well for multimodal problems [46].

In this paper, multimodal continuous ant colony optimization is introduced for multisensor remote sensing image registration. ACO can preserve high diversity and is more robust for the problem which has many local optima [40]. ACO also can keep learning during the optimization procedure [25]. Meanwhile, multimodal continuous ACO can deal with difficult multimodal problems effectively [39]. These reasons all motivate us to propose a multisensor remote sensing image registration method based on multimodal continuous ACO. DTV [22,21], which is one of the state-of-the-art registration methods, is used as similarity measure because of its robustness of intensity distortion. Meanwhile, we introduce the general DTV optimization method as an efficient local search operation according to the problem. Our method is evaluated on many multisensor images (optical images and SAR images). Experimental results show that our approach achieves the promising performance.

2. Background

2.1. Image registration

In this paper, we focus on the parametric intensity-based registration methods [42]. Let R be the reference image, and S be the source image to be registered. Then, image registration problem can be formulated as:

$$T = \underset{T}{arg\ min}\ C(R, S(T)) \tag{1}$$

where C measures the dissimilarity between the reference image R and the source image S, T represents the parameter vector of the transformation model, and $S(T)$ is the transformation image respect to T. The best transformation parameter vector is obtained when the value of dissimilarity function is minimum. Accurate registration result is based on the dissimilarity function, so accurate dissimilarity measure is necessary.

2.2. Ant colony optimization

In the 1990's, ant colony optimization was introduced as a heuristic approach inspired by the foraging behavior of ant in the nature [9]. Without visual cues, ants can find the shortest path to food source by depositing pheromone information. At first, ACO solves the traveling salesman problem (TSP) effectively [8], and then ACO is developed to solve various hard problems [10]. The general framework of ACO is shown in Algorithm 1. In the general ACO, there are three main steps: AntBasedSolutionConstruction, PheromoneUpdate, and DaemonAction. These procedures will be described in detail in the next part. Due to its efficiency, it has been applied to a range of various continuous optimization problems. ACO_R [38] is a famous and efficient version of continuous ACO, and the discrete probability distribution is shifted to a continuous form.

Algorithm 1. The general framework of ACO.

while the termination condition is not met **do**
  AntBasedSolutionConstruction
  PheromoneUpdate
  DaemonAction **end while**

2.2.1. Ant based solution construction

In the ACO_R, the construction of new solutions built by ants is completed in an incremental way from variable by variable [38]. First, the ant probabilistically selects one solution from the archive that contains the found better solutions. The probability of each solution in the archive is calculated through its weight. The weight of each solution is calculated by:

$$w_j = \frac{1}{\sigma NP\sqrt{2\pi}} e^{-\frac{(rank(j)-1)^2}{2\sigma^2 NP^2}} \tag{2}$$

where $rank(j)$ is the rank of the jth best solution in the archive, NP is the size of archive, and σ is the parameter that adjusts the importance of the rank. The large σ indicates the uniform probability distribution of the solutions in the archive, and small σ increases the performance of the top-ranked solutions. Meanwhile, the probability p_j of the solution j is defined as:

$$p_j = \frac{w_j}{\sum_{i=1}^{NP} w_i} \tag{3}$$

where NP is the size of archive.

When the solutions are selected, the ant generates the values of variables using Gaussian distribution defined as follow:

$$g(x^d, \mu^d, \delta^d) = \frac{1}{\delta^d\sqrt{2\pi}} e^{-\frac{(x^d-\mu^d)^2}{2(\delta^d)^2}} \tag{4}$$

where d is the dimension of the variables. And, δ is calculated by:

$$\delta^d = \xi \sum_{NP}^{i=1} \frac{|x_i^d - x_j^d|}{NP - 1} \tag{5}$$

where ξ is the parameter that adjusts the convergence speed. The large ξ will decrease the convergence speed, and the small ξ will accelerate convergence. The new solutions are generated through the above operations. This Solution Construction form can keep high diversity, and it is effective for multimodal optimization such as multisensor remote sensing image registration.

2.2.2. Pheromone update

Different from discrete ACO, ACO_R does not have general pheromone matrix and pheromone updating strategies. In ACO_R, the weights of the solutions are similar to the pheromone. The solution with large weight has large probability to be selected. When NP new solutions are generated, these new solutions are mixed with the solutions in the archive. Then, NP best solutions are chosen to constitute the archive. This procedure acts as the updating strategy of the pheromone, and the search is always towards the better solutions.

2.2.3. Daemon action

After the solution archive is updated, the best solution found so far is updated. In the original ACO_R, the best solution found is returned when the termination condition is met, and it also indicates that any local search operation can easily improve the performance of the algorithm [38]. In the proposed method, an efficient local search is adopted to increase the accuracy of the result.

2.3. Image registration with differential total variation

Differential total variation (DTV) is used for image registration in [22]. DTV is designed as similarity measure to match the edges of two images. This method is inspired from the intuition that the edge feature is more robust and the edge features of the two registered images are corresponding. The image gradients are calculated to denote the edge features. The locations of the image gradients should be similar, and the gradients of the residual image are encouraged to be sparse. So, any misalignments will generate ghost and increase the spareness for residual image [33]. The DTV function for image registration is formulated as:

$$\min_T E(T) = \|\nabla R - \nabla S(T)\| \tag{6}$$

where $\nabla R = \sqrt{(\nabla_1 R)^2 + ((\nabla_2 R)^2}$ denotes the gradient along the two spatial directions, and ∇_1 and ∇_2 denote the forward finite difference operators on the first and second coordinates. The DTV modal is entirely parameter free and the computation complexity is relatively low. As described in [21], DTV is more accurate and robust than MI [29] and RC [31], and DTV is one of the state-of-the-art registration similarity measures for dealing with multimodal images [21]. We compare DTV with MI on a pair of multisensor remote sensing images (Fig. 2), and it consists of one optical image and one SAR image. There are large intensity distortions and a lot of local deformations. The source image is registered with the reference image with respect to the horizontal translation. From the Fig. 2(c), it shows that DTV is much more robust than MI on this situation.

3. The proposed algorithm

In this study, the framework of adaptive multimodal continuous ACO (AM-ACO) is used as the global optimization method. AM-ACO is proposed to deal with multimodal optimization. It takes the advantage of ACO_R in preserving high diversity and avoiding premature convergence. Then, the original optimization strategy of DTV is introduced as the local search operation.

3.1. Multimodal continuous ACO

AM-ACO takes the advantages of ACO_R, and it can preserve high diversity and perform well for multimodal optimization [46]. AM-ACO focuses on multimodal optimization, so it directly utilizes the clustering based niching methods to partition the archive into several niches [35,11]. In this paper, a clustering framework for crowding is utilized as niching method (Algorithm 2), and we suppose that NP is the size of archive and NS is the size of niche. Meanwhile the ant colony size is same to the size of archive, and each niche is assigned NS ants to construct NS new solutions in each iteration.

Algorithm 2. Clustering framework for crowding.

Input: the archive, the size of niche NS
Step 1: Generate a random reference point and compute its distance to the individuals in the archive.
Step 2: Select the nearest individuals to the reference point in the archive
Step 3: Build a niche containing this individuals and $NS - 1$ individuals nearest to it.
Step 4: Eliminate these NS individuals from archive. Go to **Step 2**, if archive is not empty.
Output: a set of niches.

The parameter σ of continuous ACO plays an important role in the solution construction and convergence [38]. Large σ leads to the similar weights of the solutions, and small σ leads to bias to the better solutions. In the AM-ACO, it indicates that σ should be adjusted for different niches, and an adaptive adjusting strategy for σ is designed as:

$$\sigma_i = 0.1 + 0.3e^{-\frac{FS_{max}^i - FS_{min}^i}{FS_{max} - FS_{min} + \eta}} \tag{7}$$

where σ_i is value of σ for the ist niche, $FS_{max}{}^i$ and $FS_{min}{}^i$ are the maximum and minimum fitness values of the ist niche, FS_{max} and FS_{min} are the maximum and minimum fitness values of the archive,

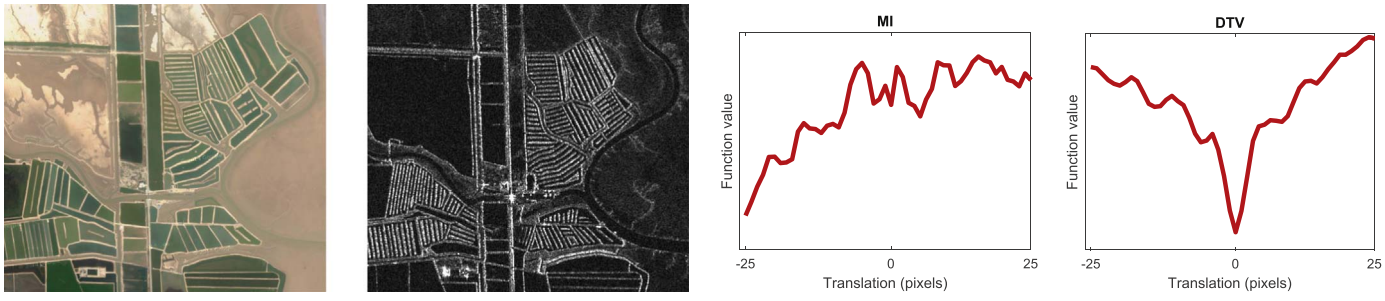

Fig. 2. An example of multisensor remote sensing image registration with respect to horizontal translation for MI and DTV. (a) Optical image. (b) SAR image. (c) Similarity measure of MI. (d) Similarity measure of DTV.

and η is a small value that avoids the denominator being zero. In this paper, η is set to 10^{-4}.

In the AM-ACO, a differential evolution (DE) mutation operator is introduced to escape from the local optima. In this paper, we introduce a global version compared to the AM-ACO. The local search operation used in the AM-ACO can converge to local optimum efficiently sometimes, so we modify the DE mutation operator to improve global search ability. The modified version is defined as follows:

$$\mu^d = x_j^d + F(x_{best}^d - x_j^d) \tag{8}$$

where $x_j{}^d$ is the dth dimension of the selected solution x_j, $x_{best}{}^d$ is the dth dimension of the best solution so far, and F is the random number within [0,1]. In the modified version, the best solution of niche is replaced by the best solution of the archive. This can provide more chances for ant to increase search areas and find more promising areas. This solution construction scheme and the traditional schemes are all performed to construct solutions. In order to take advantage of these two schemes, they are performed in the same probability.

3.2. Local search

Due to the nonlinearity of the transformation parameters, Eq. (6) is difficult to be solved directly. So local first order Taylor approximation is used as follow:

$$\nabla S(T + \triangle T) = \nabla S \bigcirc (T + \triangle T) \approx \nabla S \bigcirc T + \Im \otimes \triangle T \tag{9}$$

where $\bigcirc$ denotes the transformation operation respect to transformation parameters T, $\Im$ denotes the Jacobian, and $\Im = \frac{\partial}{\partial T}(\nabla S \bigcirc T)$. Then, the energy function Eq. (6) can be minimized with respect to $\triangle T$ as follow:

$$E(T + \triangle T) = \|\nabla R - \nabla S \bigcirc T - \Im \otimes \triangle T\|_1 \tag{10}$$

The above equation is not smooth, so the calculation of absolute value has a tight approximation as:

$$|x| = \sqrt{x^2 + \epsilon} \tag{11}$$

where ϵ is a small value, and ϵ is set to 10^{-10} in this paper. Then we can obtain the gradient of the energy function used the chain rule:

$$\nabla E(\triangle T) = \Im^T \otimes \frac{r}{\sqrt{r \bigcirc r + \epsilon}} \tag{12}$$

where $r = \nabla R - \nabla S \bigcirc T - \Im \otimes \triangle T$, and $\bigcirc$ denotes the Hadamard product.

In the local search operation, the energy function is minimized through gradient descent with backtracking. The local search operation is shown in Algorithm 3. From the Algorithm 3, we can see that this local search operation can converge to local optimum. The computational complexity of each iteration is $O(M)$, where M is the number of overlapping pixels. We do not need to perform local search operation to each new solution. Only the new solution which is better than the best solution in the archive is performed local search operation once, then this solution will be added to the archive.

Algorithm 3. Local search operation.

Input: R, S, T, μ^0, η.
Step 1: Transform S with parameters T;
Step 2: $\mu = \mu^0$;
Step 3: $\triangle T = -\mu \nabla E(0)$;
Step 4: If $E(\triangle T) > E(0)$,
$\mu = \eta\mu$
End and go to **Step 3**;
Step 5: Update transformation parameters: $T = T + \triangle T$;
Step 6: Stop if the termination criterion is met. Otherwise go to **Step 1**.
Output: T.

4. Experimental study

In this section, we evaluate the performance of the proposed method on three sets of multisensor images (optical images and SAR images). We compare our algorithm with CLPSO (comprehensive learning particle swarm optimization) [24], DE [5] and ACO [23]. CLPSO is a famous version of PSO for multimodal problems. Our method is called LMACO, which is short for multimodal continuous ACO with local search.

4.1. Experimental settings

All the experiments are operated on a computer with an Intel Core i3 3.70 GHz processor and 8.0 GB of physical memory. For comparing methods, the population size is set to 50, and the maximum number of generations is set to 100. For other parameters, we use the parameters that the authors set in the paper. All the algorithms are compiled by MATLAB.

In this paper, affine transformation is used for all experiments. Remote sensing images are usually taken by airplanes or satellites, so the deformations of transformation model between the images will not be very difficult. The affine transformation is effective and widely used for remote sensing image registration [6].

4.2. Results on the Sardinia dataset

First, we evaluate all the methods on the Sardinia dataset as Fig. 3. It consists of one TM image and one optical image. The TM image is the near-infrared band of the Landsat-5 TM image acquired in September 1995 (Fig. 3(a)), and the optical one is obtained from Google Earth in

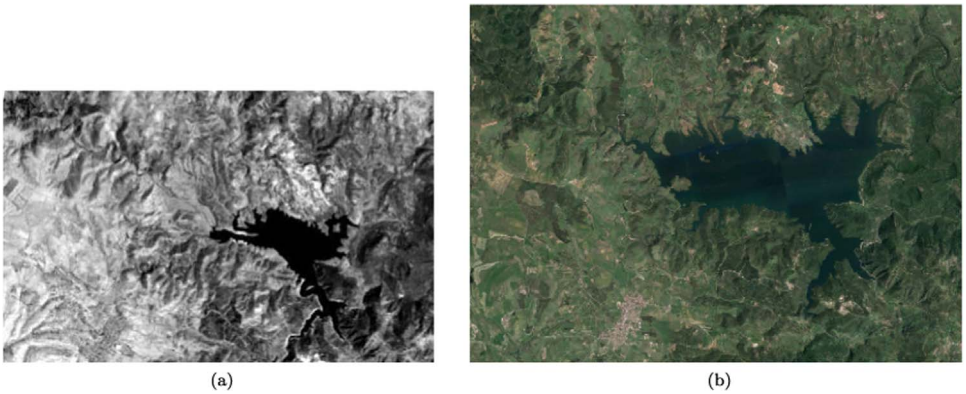

(a) (b)

Fig. 3. Sardinia dataset. (a) Near-infrared band of the Landsat-5 TM image acquired in September 1995. (b) Optical image obtained from Google Earth in July 1996.

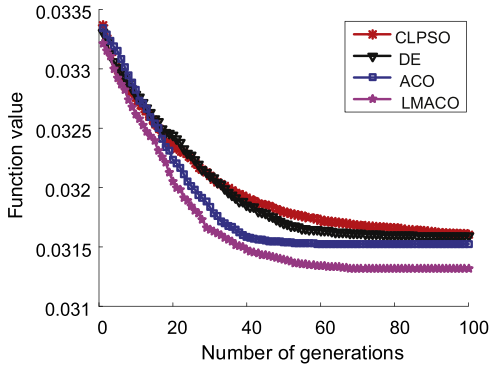

Fig. 4. The best fitness value obtained versus the number of generations.

July 1996, including red, green, and blue bands (Fig. 3(b)). Both of them share the same spatial resolution of 30 m. Two images have some misalignment, and the main difference of the overlapping area is the expansion of Lake Mulargia, on the island of Sardinia, Italy. These two images have a lot of local deformations, and the main rough sketch does not have large changes. Two images have some translation and rotation transformations. As the sardinia dataset does not have large changes between two images, it can verify the performance of all comparing methods.

In order to conduct quantitative comparison, we perform all the optimization algorithm with DTV. The result of each generation is presented in Fig. 4, and all the results are averaged over 30 independent runs. From the figure, we can see the best solutions obtained under 100 generations. Due to the local search operation, the proposed method has received the better result. ACO has high diversity and is robust than DE and CLPSO, so it can get more accurate result with the increase of the generation. CLPSO presents faster convergence speed, and CLPSO and DE all fall into local optimum.

4.3. Results on the island town dataset

Then, island town dataset is utilized (Fig. 5). Island town data set consists of two images (one SAR image and one optical image) which cover the island town in Yingkou City, Liaoning Province, China. The SAR image is obtained from the C-band of Radarsat-2 image acquired in June 2008, and the optical image is obtained from Google Earth on June 9, 2013. These two images have the same spatial resolution of 8 m. From the Fig. 5, we can see that there are a lot of detail changes, and a large rotation transformation and small scale transformation exist. Different from Sardinia dataset, two images have more local changes, and the image intensity is quite different.

MI and DTV are all calculated for all methods, and RMSE is utilized to measure the results. For LMACO with MI, the optimization strategy in [12] is utilized as local search operation. RMSE is obtained from the difference between the result and the manual ground truth. The manual ground truth is the transformation parameter obtained through the corresponding feature points which are selected manually. In all the experiments, 30 pairs of feature points are selected to calculate RMSE. Table 1 records the results on the island town dataset. The proposed method LMACO with DTV receives the lowest value of RMSE, and LMACO with MI receives the lowest value of MI. ACO obtains more accurate results than DE and CLPSO. Due to the novel learning strategy of CLPSO, CLPSO can obtain more accurate result than DE.

Table 1
The result on the island town dataset.

	MI		DTV		RMSE	
	Mean	Best	Mean	Best	Mean	Best
CLPSO with MI	−1.0120	−1.0132	0.0934	0.0929	7.142	4.956
DE with MI	−1.0119	−1.0128	0.0957	0.0945	8.625	5.645
ACO with MI	−1.0127	−1.0131	0.0931	0.0923	5.158	3.387
LMACO with MI	−1.0138	−1.0141	0.0925	0.0907	4.854	2.158
LMACO with DTV	−1.0125	−1.0129	0.0897	0.0893	1.765	0.987

4.4. Results on the Shuguang village dataset

Finally, the third dataset is composed of one SAR image and one RGB optical image as shown in Fig. 6, respectively. This dataset covers a piece of the farmland in the Shuguang Village of the Dongying City in China. Between these two images, some new buildings are built on the farmland, and the rotation transformation is large. These differences all will influence the accuracy of the comparing methods heavily. The SAR and optical images were acquired in June 2008 and September 2012, respectively.

Table 2 records the results on the shuguang village dataset. The proposed LMACO receives the better result than ACO because of the multimodal strategy and local search operation. ACO performs more robust and stable than CLPSO and DE. Meanwhile, DTV is more accurate to reflect registration result than MI.

5. Conclusion

In this paper, we introduce multimodal ACO algorithm for multisensor remote sensing image registration, and efficient local search operation is added. Due to the large differences of different imaging sensors, multisensor remote sensing image registration is a challenging

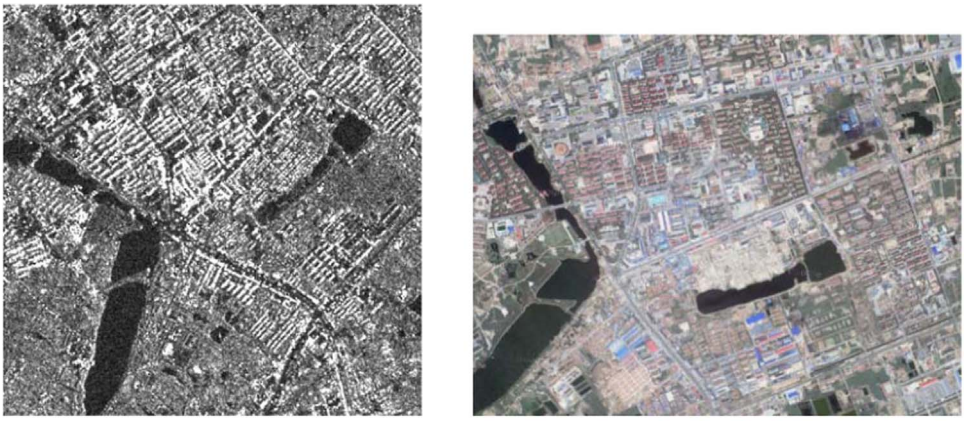

(a) (b)

Fig. 5. Island town dataset. (a) C-band of Radarsat-2 image acquired in June 2008. (b) Optical image acquired on June 9, 2013.

(a) (b)

Fig. 6. Shuguang village dataset. (a) SAR image acquired in 2008, (b) Optical image acquired in 2012.

Table 2
The result on the Shuguang village dataset.

	MI		DTV		RMSE	
	Mean	Best	Mean	Best	Mean	Best
CLPSO with MI	−1.0308	−1.0322	0.0704	0.0689	7.787	2.265
DE with MI	−1.0301	−1.0315	0.0708	0.0697	8.625	2.437
ACO with MI	−1.0315	−1.0324	0.0696	0.0681	4.985	2.215
LMACO with MI	−1.0338	−1.0351	0.0684	0.0673	3.948	1.434
LMACO with DTV	−1.0328	−1.0331	0.0671	0.0662	1.521	0.672

work. General methods usually obtain local optimum, since it is a multimodal problem and sensitive to the initial position. Multimodal ACO algorithm can preserve high diversity and has the global search ability for multimodal problems. Meanwhile, efficient local search operation can improve the efficiency and provide the accurate result. The experimental results have demonstrated the effectiveness and robustness of the proposed method. In the near future, we will consider to propose the similarity measure based on deep neural network for multisensor image registration.

References

[1] I. Ariyasingha, T. Fernando, Performance analysis of the multi-objective ant colony optimization algorithms for the traveling salesman problem, Swarm Evolut. Comput. 23 (2015) 11–26.
[2] Y. Bentoutou, N. Taleb, K. Kpalma, J. Ronsin, An automatic image registration for applications in remote sensing, IEEE Trans. Geosci. Remote Sens. 43 (9) (2005) 2127–2137.
[3] L.G. Brown, A survey of image registration techniques, ACM Comput. Surv. 24 (4) (1992) 325–376.
[4] X. Dai, S. Khorram, The effects of image misregistration on the accuracy of remotely sensed change detection, IEEE Trans. Geosci. Remote Sens. 36 (5) (1998) 1566–1577.
[5] I. De Falco, A. Della Cioppa, D. Maisto, E. Tarantino, Differential evolution as a viable tool for satellite image registration, Appl. Soft Comput. 8 (4) (2008) 1453–1462.
[6] F. Dellinger, J. Delon, Y. Gousseau, J. Michel, F. Tupin, Sar-sift: a sift-like algorithm for sar images, IEEE Trans. Geosci. Remote Sens. 53 (1) (2015) 453–466.
[7] M. Dorigo, C. Blum, Ant colony optimization theory: a survey, Theor. Comput. Sci. 344 (2) (2005) 243–278.
[8] M. Dorigo, L.M. Gambardella, Ant colony system: a cooperative learning approach to the traveling salesman problem, IEEE Trans. Evolut. Comput. 1 (1) (1997) 53–66.
[9] M. Dorigo, V. Maniezzo, A. Colorni, Ant system: optimization by a colony of cooperating agents, IEEE Trans. Syst. Man Cybern. Part B: Cybern. 26 (1) (1996) 29–41.
[10] A. Ezzat, A.M. Abdelbar, D.C. Wunsch II, A bare-bones ant colony optimization algorithm that performs competitively on the sequential ordering problem, Memet. Comput. 6 (1) (2014) 19–29.
[11] W. Gao, G.G. Yen, S. Liu, A cluster-based differential evolution with self-adaptive strategy for multimodal optimization, IEEE Trans. Cybern. 44 (8) (2014) 1314–1327.
[12] M. Gong, S. Zhao, L. Jiao, D. Tian, S. Wang, A novel coarse-to-fine scheme for automatic image registration based on sift and mutual information, IEEE Trans. Geosci. Remote Sens. 52 (7) (2014) 4328–4338.
[13] M. Gong, Z. Zhou, J. Ma, Change detection in synthetic aperture radar images based on image fusion and fuzzy clustering, IEEE Trans. Image Process. 21 (4) (2012) 2141–2151.
[14] Y. Han, F. Bovolo, L. Bruzzone, Edge-based registration-noise estimation in vhr multitemporal and multisensor images, IEEE Geosci. Remote Sens. Lett. 13 (9) (2016) 1231–1235.
[15] Y. Han, F. Bovolo, L. Bruzzone, Segmentation-based fine registration of very high resolution multitemporal images, IEEE Trans. Geosci. Remote Sens. 55 (5) (2017) 2884–2897.
[16] H. Ismkhan, Effective heuristics for ant colony optimization to handle large-scale problems, Swarm Evolut. Comput., 2016.
[17] J. Kim, J.A. Fessler, Intensity-based image registration using robust correlation coefficients, IEEE Trans. Med. Imaging 23 (11) (2004) 1430–1444.
[18] S. Klein, M. Staring, K. Murphy, M.A. Viergever, J.P. Pluim, Elastix: a toolbox for intensity-based medical image registration, IEEE Trans. Med. Imaging 29 (1) (2010) 196–205.
[19] H. Li, B. Manjunath, S.K. Mitra, Multisensor image fusion using the wavelet transform, Graph. Models Image Process. 57 (3) (1995) 235–245.
[20] Q. Li, G. Wang, J. Liu, S. Chen, Robust scale-invariant feature matching for remote sensing image registration, IEEE Geosci. Remote Sens. Lett. 6 (2) (2009) 287–291.
[21] Y. Li, C. Chen, F. Yang, J. Huang, Deep sparse representation for robust image registration, in IEEE Conference on Computer Vision and Pattern Recognition, 2015, pp. 4894–4901.
[22] Y. Li, C. Chen, J. Zhou, J. Huang, Robust image registration in the gradient domain, in IEEE International Symposium on Biomedical Imaging (ISBI), 2015, pp. 605–608.
[23] J. Liang, X. Liu, K. Huang, X. Li, D. Wang, X. Wang, Automatic registration of multisensor images using an integrated spatial and mutual information (smi) metric, IEEE Trans. Geosci. Remote Sens. 52 (1) (2014) 603–615.
[24] J.J. Liang, A.K. Qin, P.N. Suganthan, S. Baskar, Comprehensive learning particle swarm optimizer for global optimization of multimodal functions, IEEE Trans. Evolut. Comput. 10 (3) (2006) 281–295.
[25] T. Liao, K. Socha, M.A.M. de Oca, T. Stützle, M. Dorigo, Ant colony optimization for mixed-variable optimization problems, IEEE Trans. Evolut. Comput. 18 (4) (2014) 503–518.
[26] D.G. Lowe, Object recognition from local scale-invariant features, in IEEE International Conference on Computer Vision, vol. 2, 1999, pp. 1150–1157.
[27] D.G. Lowe, Distinctive image features from scale-invariant keypoints, Int. J. Comput. Vision. 60 (2) (2004) 91–110.
[28] W. Ma, Z. Wen, Y. Wu, L. Jiao, M. Gong, Y. Zheng, L. Liu, Remote sensing image registration with modified sift and enhanced feature matching, IEEE Geosci. Remote Sens. Lett. PP (99) (2016) 1–5.
[29] F. Maes, A. Collignon, D. Vandermeulen, G. Marchal, P. Suetens, Multimodality image registration by maximization of mutual information, IEEE Trans. Med. Imaging 16 (2) (1997) 187–198.
[30] J.M. Murphy, J. Le Moigne, D.J. Harding, Automatic image registration of multimodal remotely sensed data with global shearlet features, IEEE Trans. Geosci. Remote Sens. 54 (3) (2016) 1685–1704.
[31] A. Myronenko, X. Song, Intensity-based image registration by minimizing residual complexity, IEEE Trans. Med. Imaging 29 (11) (2010) 1882–1891.

[32] K.V. Narasimha, E. Kivelevitch, B. Sharma, M. Kumar, An ant colony optimization technique for solving min-max multi-depot vehicle routing problem, Swarm Evolut. Comput. 13 (2013) 63–73.
[33] D. Needell, R. Ward, Stable image reconstruction using total variation minimization, SIAM J. Imaging Sci. 6 (2) (2013) 1035–1058.
[34] R. Panda, S. Agrawal, M. Sahoo, R. Nayak, A novel evolutionary rigid body docking algorithm for medical image registration, Swarm Evolut. Comput. 33 (2016) 108–118.
[35] B.-Y. Qu, P.N. Suganthan, J.-J. Liang, Differential evolution with neighborhood mutation for multimodal optimization, IEEE Trans. Evolut. Comput. 16 (5) (2012) 601–614.
[36] K.M. Salama, A.A. Freitas, Abc-miner+ constructing markov blanket classifiers with ant colony algorithms, Memet. Comput. 6 (3) (2014) 183–206.
[37] K.M. Salama, A.A. Freitas, Classification with cluster-based bayesian multi-nets using ant colony optimisation, Swarm Evolut. Comput. 18 (2014) 54–70.
[38] K. Socha, M. Dorigo, Ant colony optimization for continuous domains, Eur. J. Oper. Res. 185 (3) (2008) 1155–1173.
[39] N. Sreeja, A. Sankar, A hierarchical heterogeneous ant colony optimization based approach for efficient action rule mining, Swarm Evolut. Comput. 29 (2016) 1–12.
[40] A. Swarnkar, N. Gupta, K. Niazi, Adapted ant colony optimization for efficient reconfiguration of balanced and unbalanced distribution systems for loss minimization, Swarm Evolut. Comput. 1 (3) (2011) 129–137.
[41] K. Takita, Y. Sasaki, T. Higuchi, K. Kobayashi, High-accuracy subpixel image registration based on phase-only correlation, IEICE Trans. Fundam. Electron. Commun. Comput. Sci. 86 (8) (2003) 1925–1934.
[42] M.P. Wachowiak, R. Smolíková, Y. Zheng, J.M. Zurada, A.S. Elmaghraby, An approach to multimodal biomedical image registration utilizing particle swarm optimization, IEEE Trans. Evolut. Comput. 8 (3) (2004) 289–301.
[43] Z. Wang, H. Xing, T. Li, Y. Yang, R. Qu, Y. Pan, A modified ant colony optimization algorithm for network coding resource minimization, IEEE Trans. Evolut. Comput. 20 (3) (2016) 325–342.
[44] J. Woo, M. Stone, J.L. Prince, Multimodal registration via mutual information incorporating geometric and spatial context, IEEE Trans. Image Process. 24 (2) (2015) 757–769.
[45] Y. Wu, W. Ma, M. Gong, L. Su, L. Jiao, A novel point-matching algorithm based on fast sample consensus for image registration, IEEE Geosci. Remote Sens. Lett. 12 (1) (2015) 43–47.
[46] Q. Yang, W.-N. Chen, Z. Yu, T. Gu, Y. Li, H. Zhang, J. Zhang, Adaptive multimodal continuous ant colony optimization, IEEE Trans. Evolut. Comput. 21 (2) (2016) 191–205.
[47] B. Zitova, J. Flusser, Image registration methods: a survey, Image Vision. Comput. 21 (11) (2003) 977–1000.